UV-Photoelectron Spectra of [M(η^3-C_3H_5)$_2$] (M = Ni, Pd, Pt) Revisited: A Quasi-Relativistic Density Functional Study

Maurizio Casarin,*,† Luciano Pandolfo,‡ and Andrea Vittadini§

Dipartimento di Chimica Inorganica, Metallorganica ed Analitica, Università di Padova, Padova, Italy, Dipartimento di Chimica, Università della Basilicata, Potenza, Italy, and Centro di Studio sulla Stabilità e Reattività dei Composti di Coordinazione del CNR, Via Loredan 4, Padova, Italy

Received October 2, 2000

The molecular and electronic structure of [M(η^3-C_3H_5)$_2$] (M = Ni, Pd, Pt) has been investigated by means of quasi-relativistic gradient-corrected density functional calculations. Geometries have been fully optimized by considering both trans and cis arrangements of the bis(η^3-allyl) moiety. Binding energy differences between isomers are always smaller than 0.2 kcal/mol; in particular, *cis*-[Ni(η^3-C_3H_5)$_2$] is computed to be more stable than *trans*-[Ni(η^3-C_3H_5)$_2$], while a reversed order is obtained for Pd and Pt analogues. Computed geometrical parameters of *trans*-[Ni(η^3-C_3H_5)$_2$] compare very well with available structural data. Moreover, a new assignment of variable energy photoelectron spectroscopy measurements [Li, X.; Bancroft, G. M.; Puddephatt, R. J.; Liu, Z. F.; Hu, Y. F.; Tan, K. H. *J. Am. Chem. Soc.* **1994**, *116*, 9543−9554] is proposed by assuming that the trans:cis ratio in the gas phase is close to one.

Introduction

The bonding interaction between metal centers (M) and unsaturated ligands (L) was first described by Dewar[1] and by Chatt and Duncanson[2] on the basis of a two-way electron flow, i.e., a L→M charge transfer from ligand σ or π molecular orbitals (MO) into suitable M virtual levels assisted by a M→L back-donation from atom-like d_π atomic orbitals (AOs) into L π^* virtual MOs.

Since then, much work has been done in order to understand how the relative degree of donation and back-donation is affected by (i) the ancillary ligands bonded to M, (ii) the nature of L, (iii) the number of d electrons localized on M, and (iv) the relativistic effects on passing from first- to second- and third-row transition metals.[3] An invaluable contribution to this effort has been certainly provided by the complementary use of quantum mechanical calculations and gas-phase UV photoelectron spectroscopy (PES). Actually, PES provides a map of the energy of the outermost occupied MOs, supplying a check of theoretical results, which, in turn, furnish information about the M−L bonding scheme.[4,5] Despite the wide success of this methodology, in a few cases the MO ordering of even simple molecules such as [M(η^3-C_3H_5)$_2$] (M = Ni, Pd, and Pt) is still an open question.[6]

[M(η^3-allyl)$_2$] can be considered as the simplest sandwich compounds, and, even if NMR data indicate that, in toluene-d_8 solutions, [Ni(η^3-C_3H_5)$_2$][7−8] (hereafter **A**) is present as a mixture of cis and trans isomers in the approximate proportion of 1:3, the crystal structure has been obtained only for the trans isomer.[9] No structural data are available for [Pd(η^3-C_3H_5)$_2$] (**B**) and [Pt(η^3-C_3H_5)$_2$] (**C**); nevertheless, their NMR spectra are consistent with the coexistence of the two isomeric forms.[10]

† Università di Padova. Fax: (0039) 049 8275161. E-mail: casarin@chim02.unipd.it.
‡ Università della Basilicata.
§ CSSRCC CNR.

(1) Dewar, M. J. S. *Bull. Soc. Chim. Fr.* **1951**, *18*, C71.
(2) Chatt, J.; Duncanson, L. A. *J. Chem. Soc.* **1953**, 2939.
(3) (a) Chatt, J.; Dilworth, J. R.; Richards, R. L. *Chem. Rev.* **1978**, *78*, 589. (b) Lukehart, C. M. *Fundamental Transition Metal Organometallic Chemistry*; Brooks/Cole: Monterey, CA, 1985. (c) Hartley, F. R. In *Comprehensive Organometallic Chemistry*; Wilkinson, G., Ed.; Pergamon: Oxford, U.K., 1982; Vol. 6. (d) Veillard, A. *Chem. Rev.* **1991**, *91*, 743. (e) Koga, N.; Morokuma, K. *Chem. Rev.* **1991**, *91*, 823. (f) Li, J.; Schreckenbach, G.; Ziegler, T. *J. Chem. Phys.* **1994**, *98*, 4838. (g) Li, J.; Schreckenbach, G.; Ziegler, T. *J. Am. Chem. Soc.* **1995**, *117*, 486. (h) Jacobsen, H.; Schreckenbach, G.; Ziegler, T. *J. Phys. Chem.* **1994**, *98*, 11406. (i) Li, J.; Schreckenbach, G.; Ziegler, T. *Inorg. Chem.* **1995**, *34*, 3245. (j) Niu, S.; Hall, M. B. *Chem. Rev.* **2000**, *100*, 353. (k) Dedieu, A. *Chem. Rev.* **2000**, *100*, 543. (l) Frenking, G.; Fröhlich, N. *Chem. Rev.* **2000**, *100*, 717.
(4) (a) Fenske, R. F. *Progr. Inorg. Chem.* **1976**, *21*, 179. (b) Furlani, C.; Cauletti, C. *Struct. Bond.* (*Berlin*) **1978**, *35*, 119. (c) Lichtenberger, D. L.; Kellog, G. E. *Acc. Chem. Res.* **1987**, *20*, 379. (d) Oskam, A. *Adv. Spectrosc.* **1987**, *14*, 429. (e) Green, J. C. *Acc. Chem. Res.* **1994**, *27*, 131. (f) Xiaorong, L.; Bancroft, G. M.; Puddephatt, R. J. *Acc. Chem. Res.* **1997**, *30*, 213. (g) Granozzi, G.; Casarin, M. In *Topics in Physical Organometallic Chemistry* Gielen M., Ed.; Freund Publishing House: 1989; Vol. 3, p 107.
(5) Fragalà, I. In *Organometallics of the f-elements*, Marks, T. J., Fisher, R. D., Eds.; D. Reidel Publishing Co.: Dordrecht, Holland, 1979; p 421.
(6) (a) Li, X.; Bancroft, G. M.; Puddephatt, R. J.; Liu, Z. F.; Hu, Y. F.; Tan, K. H. *J. Am. Chem. Soc.* **1994**, *116*, 9543, and references therein. (b) Li, X.; Bancroft, G. M.; Puddephatt, R. J.; Hu, Y. F.; Liu, Z. F.; Sutherland, D. G. J.; Tan, K. H. *J. Chem. Soc., Chem. Commun.* **1993**, 67. (c) Li, X.; Bancroft, G. M.; Puddephatt, R. J.; Hu, Y. F.; Liu, Z. F.; Tan, K. H. *Inorg. Chem.* **1992**, *31*, 5162. (d) Böhm, M. C.; Gleiter, R. *Chem. Phys, Lett.* **1986**, *123*, 87. (e) Moncrieff, D.; Hillier, I. H.; Saunders: V. R.; von Niessen, W. *J. Chem. Soc., Chem. Commun.* **1985**, 779. (f) Böhm, M. C.; Gleiter, R.; Batich, C. D. *Helv. Chim. Acta* **1980**, *6*, 990. (g) Batich, C. D. *J. Am. Chem. Soc.* **1976**, *98*, 7585.
(7) Bönnemann, H.; Bogdanović, B.; Wilke, G. *Angew. Chem., Int. Ed. Engl.* **1967**, *6*, 804.
(8) Henc, B.; Jolly, P. W.; Salz, R.; Wilke, G.; Benn, R.; Hoffmann, E. G.; Mynott, R.; Schroth, G.; Seevogel, K.; Sekutowski, J. C.; Krüger, C. *J. Organomet. Chem.* **1980**, *191*, 425.
(9) Goddard, R.; Krüger, C.; Mark, F.; Stansfield, R.; Zhang, X. *Organometallics* **1985**, *4*, 285.

10.1021/om0008427 CCC: $20.00
Publication on Web 01/20/2001

Li et al.[6a−c] investigated the electronic structure of **A**, **B**, and **C** by means of variable energy PES and Xα scattered-wave (Xα-SW) calculations, concluding that (i) the comparison of theoretical data (orbital energies and orbital character) pertaining to cis and trans complexes with experimental measurements indicates that "there is no observable cis compound (<20% of trans)" in the gas-phase PE spectra; (ii) the peak lying at the lowest IE is due to the ionization from MOs having different character along the series: in **A** it is due to the ionization from two Ni-based MOs of symmetry a_g (the symmetry point group of *trans*-[M(η^3-C_3H_5)$_2$] is the C_{2h} one), while a (η^3-C_3H_5)$_2$-based MO of symmetry a_u is involved in **B** and **C**. Incidentally, the assignment of the lowest IE band of **A** to the ionization from two metal-based MOs agrees with data reported by Batich,[6g] but it is in contrast with theoretical results published by different authors[6d−f] which ascribed the peak lying at the lowest IE to a ligand-based MO of symmetry a_u.

Undoubtedly, Li et al.[6a−c] issued a large amount of experimental data, but the theoretical part of their work suffers of some flaws, i.e., (i) the inaccurate description of the electron density, typical of Xα-SW calculations; (ii) the absence of any geometry optimization;[11,12] (iii) the neglect of relativistic effects.[13] Thus, we decided to carry out new and more accurate calculations aimed at obtaining a deeper insight into the electronic structure of **A**, **B**, and **C**, and at revisiting the assignment of their gas-phase PE spectra.

Methods

The calculations herein reported have been carried out by using the density functional ADF package,[15] developed by Baerends and co-workers.[16] A triple-ζ Slater-type basis set was used for the M atoms, while a double-ζ basis was used for carbon and hydrogen valence orbitals. The inner core shells were treated by the frozen-core approximation. Nonlocal (NL) corrections to the LDA functional were self-consistently included by adopting the Becke[17a] and the Perdew[17b,c] functionals for the exchange and for the correlation parts, respectively.

C_{2h} and C_{2v} symmetries were assumed for trans and cis isomers, respectively (see Figure 1), with the C_2 axis oriented along *z* in both cases. All the numerical experiments have been performed at a quasi-relativistic level,[18] in the sense that the first-order scalar relativistic Pauli Hamiltonian is diagonalized in the space of the nonrelativistic solutions, i.e., in the nonrelativistic basis set. Finally, the M−L binding energy has been analyzed by means of the extended transition state method,[19] by considering, as interacting fragments, the central M atom and the $(C_3H_5)_2$ moiety. According to this scheme, the [M(η^3-C_3H_5)$_2$] binding energy, ΔE, may be written as

$$\Delta E = -(\Delta E_{es} + \Delta E_{Pauli} + \Delta E_{orb} + \Delta E_{prep}) \qquad (1)$$

Here, ΔE_{es}, ΔE_{Pauli}, and ΔE_{orb} represent contributions due to the pure electrostatic interaction, the Pauli repulsion (hereafter $\Delta E_{es} + \Delta E_{Pauli} = \Delta E_{sr}$, the steric repulsion), and the orbital interaction, respectively. ΔE_{orb} may be further decomposed into contributions due to different symmetry representations (γ) of the molecular point group according to

$$\Delta E_{orb} = \sum_{\gamma} \Delta E^{\gamma}_{orb} \qquad (2)$$

As far as the last term ΔE_{prep} is concerned, it provides information about the energy required to relax the structure of the free fragments to the geometry they assume in the final complex.

Crystal orbital overlap population (COOP)[20] curves have been computed by applying a Lorentzian broadening factor of 0.25 eV to the complex eigenvalues. COOP curves were obtained by weighting one-electron energy levels by their basis orbital percentage to obtain information about the localization and the bonding/antibonding character of selected MOs. Finally, IEs and attachment energies (AEs, to a first approximation the negative of the electron affinities of the capturing species) have been computed by employing the Slater transition state (TS) procedure[21] to include relaxation effects which strongly affect the ordering of cation and anion energy levels in metal complexes.

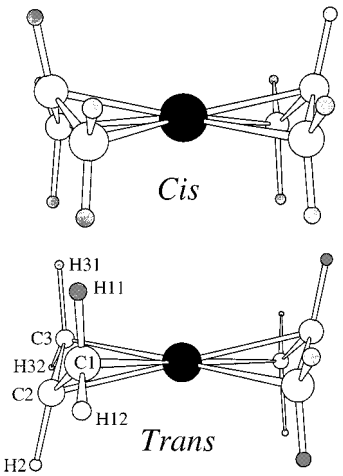

Figure 1. Schematic view of the *cis*- and *trans*-[M(η^3-C_3H_5)$_2$] complexes. In both cases, the binary axis coincides with *z*. The σ mirror planes are *xz* and *yz* for the *cis* isomer, *xy* for the trans isomer.

Results and Discussion

A selection of the optimized geometrical parameters of **A**, **B**, and **C** is reported in Table 1 together with experimental[9] bond lengths (BL) and bond angles (BA)

(10) (a) Becconsall, J. K.; Job, B. E.; O'Brien, S. *J. Chem. Soc. A* **1967**, 423. (b) O'Brien, S. *J. Chem. Soc. A* **1970**, 9.

(11) Crystallographic data are only available for *trans*-**A**[9] and *trans*-[Pd(η^3-$C_3H_4CH_3$)$_2$].[12] Geometrical parameters corresponding to *trans*-[Pd(η^3-$C_3H_4CH_3$)$_2$] were used by Li et al.[6a] for *trans*-**B** and for the (η^3-C_3H_5)$_2$ moiety of *trans*-**C**, while the distance between the Pt atom and the allyl plane was increased by 0.04 Å. As a consequence of the lack of structural data for the cis isomers, the corresponding geometries were generated by simply performing a reflection operation on one allyl-ligand of the trans forms.[6a]

(12) Gozum, J. E.; Pollina, D. M.; Jensen, J. A.; Girolami, G. S. *J. Am. Chem. Soc.* **1988**, *110*, 2688.

(13) Relativistic effects are known to be very important for 5d elements.[14] The mass increase of s electrons with high instantaneous velocities near the nucleus has the effects of contracting and stabilizing the s orbitals, thus destabilizing the 5d levels whose electrons experience a reduced effective nuclear charge.

(14) Pyykkö, P.; Declaux, J.-P. *Acc. Chem. Res.* **1979**, *12*, 276.

(15) ADF 1999, Department of Theoretical Chemistry, Vrije Universiteit: Amsterdam, 1999.

(16) (a) Post, D.; Baerends, E. J. *J. Chem. Phys.* **1983**, *78*, 5663. (b) Baerends, E. J.; Ellis, D. E.; Ros, P. *Chem. Phys.* **1973**, *2*, 41.

(17) (a) Becke, A. *Phys. Rev. A* **1988**, *38*, 3098. (b) Perdew, J. P. *Phys. Rev. B* **1986**, *33*, 8822. (c) Perdew, J. P. *Phys. Rev. B* **1986**, *34*, 7406.

(18) Ziegler, T.; Tschinke, V.; Baerends, E. J.; Snijders, J. G.; Ravenek, W. *J. Phys. Chem.* **1989**, *93*, 3050.

(19) Ziegler, T.; Rauk, A. *Theor. Chim. Acta* **1977**, *46*, 1.

(20) Hoffmann, R. *Solids and Surfaces: A Chemist's View of Bonding in Extended Structures*; VCH: New York, 1988.

(21) Slater, J. C. *Quantum Theory of Molecules and Solids. The Self-Consistent-Field for Molecules and Solids*; McGraw-Hill: New York, 1974; Vol. 4.

Table 1. Selected Structural Parameters for *trans*-[M(η^3-C_3H_5)$_2$] and *cis*-[M(η^3-C_3H_5)$_2$] (M = Ni, Pd, Pt)[a]

	trans			cis		
	Ni	Pd	Pt	Ni	Pd	Pt
			BL (Å)			
M−C2	1.977 (1.980)	2.144	2.143	1.968	2.135	2.126
M−C1	2.026 (2.031)	2.197	2.189	2.026	2.195	2.184
M−C3	2.026 (2.027)	2.197	2.189	2.026	2.195	2.184
C1−C2	1.416 (1.414)	1.416	1.423	1.417	1.417	1.426
C2−H2	1.100 (1.093)	1.100	1.098	1.100	1.100	1.098
C1−H12	1.094 (1.093)	1.093	1.093	1.093	1.093	1.093
C1−H11	1.098 (1.091)	1.096	1.096	1.100	1.097	1.096
C3−H32	1.094 (1.094)	1.093	1.093	1.093	1.093	1.093
C3−H31	1.098 (1.086)	1.096	1.096	1.100	1.097	1.096
			BA (deg)			
C1−M−C3	74.7 (74.6)	68.5	68.8	74.7	68.6	69.0
C1−M−C2	41.4 (41.2)	38.0	38.3	41.5	38.2	38.5
C3−M−C2	41.4 (41.4)	38.0	38.3	41.5	38.2	38.5
C2−C1−H11	120.0 (120.4)	120.0	119.7	119.9	120.0	119.9
C2−C1−H12	119.0 (119.6)	118.8	118.2	119.2	118.8	118.0
C1−C2−H2	118.6 (118.2)	118.3	118.7	118.6	118.2	118.7
C3−C2−H2	118.6 (118.9)	118.3	118.7	118.6	118.2	118.7
C2−C3−H31	120.0 (120.3)	120.0	119.7	119.9	120.0	119.9
C2−C3−H32	119.0 (119.5)	118.8	118.2	119.2	118.8	118.0
C1−C2−C3	120.4 (120.5)	121.7	120.7	120.3	121.8	120.3
M−C1−H11	101.7 (99.1)	102.3	104.5	102.3	102.7	105.4
M−C1−H12	122.9 (122.9)	121.4	120.4	122.7	121.4	120.2
M−C2−H2	114.8 (114.8)	113.3	112.9	114.0	112.9	112.6
M−C3−H31	101.7 (100.1)	102.3	104.5	102.3	102.7	105.4
M−C3−H32	122.9 (123.3)	121.4	120.4	122.7	121.4	120.2
H11−C1−H12	115.5 (115.9)	115.6	115.6	115.5	115.5	115.5
H31−C3−H32	115.5 (115.5)	115.6	115.6	115.5	115.5	115.5
ΔE_{isom}	0.00	0.00	0.00	−0.10	0.14	0.06

[a] Bond lengths (BL) and bond angles (BA) are in Å and deg, respectively. Crystallographic data pertaining to *trans*-[Ni(η^3-C_3H_5)$_2$] (Goddard, R.; Krüger, C.; Mark, F.; Stansfield, R.; Zhang, X. *Organometallics* **1985**, *4*, 285−290) are reported in parentheses for comparison. Taking the trans form as a reference, the ΔE_{isom} (in kcal/mol) between the two forms is also included. Refer to Figures 1 and 2 for the atom labeling.

of *trans*-**A**. Moreover, the relationship of hydrogen atoms to the carbon skeleton of cis and trans (η^3-C_3H_5)$_2$ fragments is displayed in Figure 2. In detail, this figure shows the degree of bending of C−H bonds out of the plane defined by C1, C2, and C3, with a negative sign meaning a bend toward the M atom, which parenthetically lies 1.5/1.7 Å from this plane. As in Table 1, experimental data pertaining to *trans*-**A** are also included for comparison. We point out that (i) the agreement with experiment[9] is very good; (ii) BLs and BAs are very similar for *trans*- and *cis*-**A**, which result also quasi-isoenergetic (see Table 1); (iii) the distance of Ni to the meso carbon atom C2 of each η^3-allyl group is significantly shorter than that to C1 and C3; (iv) the anti hydrogen atoms H11 and H31 appear to lie about 30° out of the C1−C2−C3 plane, away from the Ni atom, while H12, H2, and H32 are bent toward Ni, the meso H2 atom being bent the most.

In the past, the molecular structure of **A** has been theoretically investigated by Tobisch and Boegel[22a] as well as by Gugelchuck.[22b] Only Gugelchuck addressed the issue of the isomer relative stability, and he predicted the trans form to be favored by 0.5 kcal/mol. However, it should be remarked that such an estimate was done by performing gradient-corrected calculations on geometries optimized within the local density approximation, a procedure that can easily introduce errors of the order of the small energy difference found.

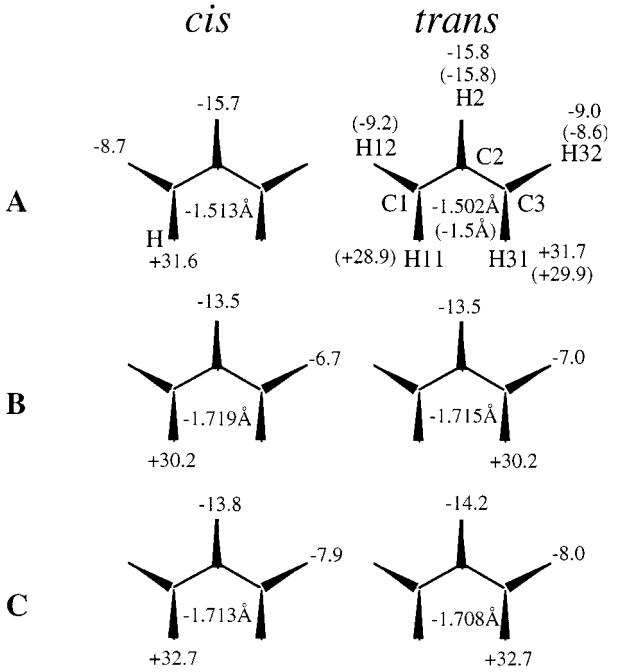

Figure 2. Optimized deviations (deg) of the hydrogen atoms out of the plane of the allyl group for *cis*- and *trans*-[M(η^3-C_3H_5)$_2$] (M = Ni, Pd, Pt). Experimental deviations of *trans*-[Ni(η^3-C_3H_5)$_2$] are also reported (in parentheses) for comparison.

As already pointed out,[11] the only structural determination of a bis-allyl Pd derivative is the one reported by Gozun et al.[12] for *trans*-[Pd(η^3-$C_3H_4CH_3$)$_2$], while no data are available for any Pt derivative. The optimization of *cis*- and *trans*-[Pd(η^3-$C_3H_4CH_3$)$_2$][23] yielded results very similar to those reported in Table 1, indicating that the effects of the methylation on the meso C2 atom are negligible. It also apparent from Table 1 that minor variations are present on passing from **B** to **C**. Finally, as already found for **A**, trans and cis isomers of **B** and **C** are almost isoenergetic.

As a whole, the results so far reported do not clearly indicate a prevalence of the trans form of **A**, **B**, and **C** in the gas phase, which, on the other hand, was assumed in the interpretation of their PE spectra.[6]

Before presenting our results, we give a brief description of the bonding scheme of [M(η^3-C_3H_5)$_2$] complexes based on symmetry arguments and overlap considerations. [M(η^3-C_3H_5)$_2$] may be thought as constituted by two interacting fragments: M and (C_3H_5)$_2$. The frontier orbitals of M are the *n*d, (*n*+1)s, and (*n*+1)p AOs, while those of the (C_3H_5)$_2$ moiety are the in-phase (+) and out-of-phase (−) linear combinations of the allyl π orbitals (π_1, π_2, π_3).[24] In the C_{2h} symmetry the M AOs transform as a_g (s, d_{xy}, $d_{x^2-y^2}$, d_{z^2}), b_g (d_{xz}, d_{yz}), a_u (p_z), and b_u (p_x, p_y), while in the C_{2v} group they span the following irreducible representations: a_1 (s, p_z, $d_{x^2-y^2}$, d_{z^2}), a_2 (d_{xy}),

(22) (a) Tobisch, S.; Boegel, H. *Int. J. Quantum Chem.* **1995**, *56*, 575. (b) Gugelchuk, M. M. *J. Mol. Struct (THEOCHEM)* **1995**, *357*, 263.

(23) Optimized BLs (Å) and BAs (deg) pertaining to *trans*-[Pd(η^3-$C_3H_4CH_3$)$_2$] compare quite well with experiment (mean values in parentheses): Pd−C1 = 2.191 (2.175), Pd−C2 = 2.144 (2.149), C1−C2 = 1.416 (1.408), C2−C4 = 1.509 (1.502), C1−C2−C3 = 118.5 (118.7), C1−C2−C4 = 120.3 (120.2), C1−C2−C3−H31 = 35.5 (34.0), C1−C2−C3−H32 = 171.9 (174). The trans isomer is computed to be favored by 0.12 kcal/mol with respect to the cis one.

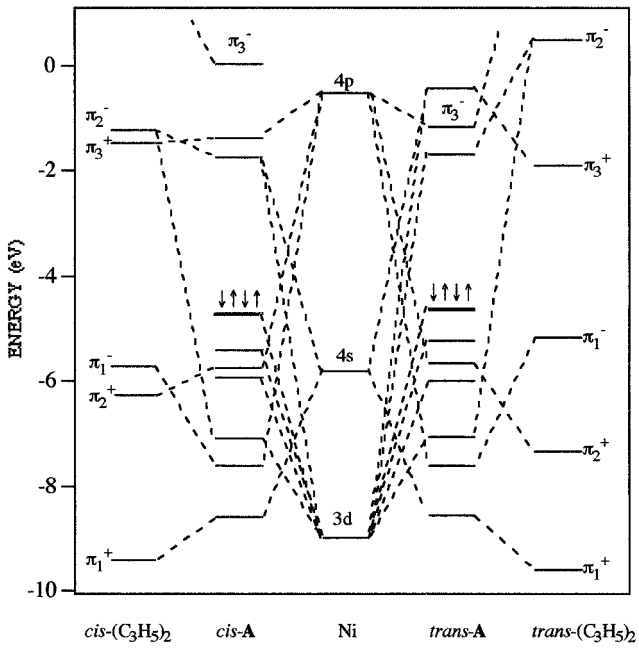

Figure 3. Interaction diagram between ground-state energy levels of Ni and π orbitals of the optimized *cis*/*trans*-$(C_3H_5)_2$ fragments.

b_1 (p_x, d_{xz}), and b_2 (p_y, d_{yz}). As far as the $(C_3H_5)_2$ fragment MOs (FMOs) are concerned, they transform in the C_{2h} (C_{2v}) symmetry as follows: π_1^+ and π_3^+ as a_g (a_1), π_1^- and π_3^- as b_u (b_1), π_2^+ as a_u (b_2), and π_2^- as b_g (a_2). In the $(C_3H_5)_2$ free fragment, π_1^+, π_1^-, and π_2^+ FMOs are occupied, while π_2^-, π_3^+, and π_3^- are empty. Hence, the valence manifold of **A**, **B**, and **C** will include eight occupied MOs (five of them with a significant localization on the M *n*d AOs) and three empty levels, reminiscent of π_2^-, π_3^+, and π_3^- $(C_3H_5)_2$ FMOs.

In Figure 3 the interaction diagram between Ni frontier orbitals and π FMOs of *cis*/*trans*-$(C_3H_5)_2$ is reported. Overall, the electronic structures of the isomers are very similar, the main difference being the inversion of π_3^+ and π_3^- orbitals on passing from the free ligand to the trans complex, which does not occur for the cis one. In this regard, it has to be emphasized that the energy of π^+ and π^- combinations reported in Figure 3 refers to the isolated and optimized *cis*- and *trans*-$(C_3H_5)_2$ fragments and that the FMO energy ordering corresponding to the isolated *cis*- and *trans*-$(C_3H_5)_2$ at the geometry it assumes in **A**, **B**, and **C** is different: for all the complexes (both cis and trans) we have $\pi_3^- > \pi_3^+ > \pi_2^- > \pi_2^+ > \pi_1^- > \pi_1^+$.

In Tables 2, 3, and 4 the charge density analysis of the frontier orbitals of cis and trans **A**, **B**, and **C** is reported. The three lowermost unoccupied MOs have been included because they can be compared with available electron transmission spectroscopy (ETS) data.[25] Slater TSIEs (TSAEs) have been computed for all the occupied (unoccupied) orbitals included in Tables 2, 3, and 4. These calculations have been always performed by employing GS geometries.

Table 2. Atomic Character for *cis*-[Ni(η³-$C_3H_5)_2$] and *trans*-[Ni(η³-$C_3H_5)_2$][a]

			population,%								
	eigenvalue		Ni			2C2		4C1			
MO	−ϵ/eV	−IE/eV	s	p	d	s	p	s	p	10H	character[b]
$8b_1$	−0.03	−2.61	0	0	6	0	39	2	42	11	π_3^-
$10a_1$	1.38	−1.25	4	14	9	0	40	0	27	6	π_3^+
$5a_2$[a]	1.74	−1.12	0	0	34	0	0	2	60	4	$(d_{xy}-\pi_2^-)^{ab}$
$9a_1$	4.72	8.80	6	0	89	0	3	0	1	1	d_{z^2}
$6b_2$	4.73	8.15	0	2	89	0	0	0	7	2	d_{yz}
$7b_1$	5.41	9.20	0	0	86	0	0	0	8	6	$d_{xz}\rightarrow\pi_3^-$
$5b_2$	5.76	8.56	0	10	8	0	1	1	78	2	π_2^+
$8a_1$	5.95	9.60	2	0	82	0	4	1	9	2	$d_{x^2-y^2}\rightarrow\pi_3^+$
$4a_2$	7.11	10.21	0	0	55	0	7	0	35	3	$(d_{xy}-\pi_2^-)^b$
$6b_1$	7.63	10.40	0	7	2	1	41	0	37	12	π_1^-
$7a_1$	8.60	11.29	7	0	0	0	28	0	40	25	π_1^+
$10a_g$	0.44	−2.01	16	0	13	0	43	−1	23	6	π_3^+
$8b_u$	1.18	−1.42	0	17	0	0	33	1	40	9	π_3^-
$6b_g$[a]	1.69	−1.20	0	0	36	0	0	2	59	3	$(d_{xz}-\pi_2^-)^{ab}$
$9a_g$	4.61	8.72	6	0	90	0	1	0	2	1	$d_{x^2-y^2}+d_{z^2}+d_{xy}$
$5b_g$	4.74	8.99	0	0	97	0	0	0	1	2	d_{yz}
$8a_g$	5.22	9.22	1	0	92	0	1	0	1	5	$d_{xy}+d_{x^2-y^2}+d_{z^2}$
$5a_u$	5.67	8.43	0	11	0	0	1	1	84	3	π_2^+
$7a_g$	6.00	9.63	2	0	80	0	4	0	12	2	$d_{z^2}+d_{xy}+d_{x^2-y^2}\rightarrow\pi_3^+$
$4b_g$	7.07	10.18	0	0	54	0	6	0	36	4	$(d_{xz}-\pi_2^-)^b$
$7b_u$	7.61	10.39	0	7	0	1	42	0	39	11	π_1^-
$6a_g$	8.56	11.23	7	0	0	0	27	0	38	28	π_1^+

[a] Lowest unoccupied MO. [b] b and ab stand for bonding and antibonding, respectively.

Table 3. Atomic Character for *cis*-[Pd(η³-$C_3H_5)_2$] and *trans*-[Pd(η³-$C_3H_5)_2$][a]

			population,%								
	eigenvalue		Pd			2C2		4C1			
MO	−ϵ/eV	−IE/eV	s	p	d	s	p	s	p	10H	character[b]
$8b_1$	0.18	−2.34	0	0	6	0	41	2	41	10	π_3^-
$10a_1$	1.24	−1.18	7	18	7	−1	39	0	23	7	π_3^+
$5a_2$[a]	1.66	−1.09	0	0	31	0	0	2	63	4	$(d_{xy}-\pi_2^-)^{ab}$
$6b_2$	5.23	7.92	0	4	17	0	1	2	73	3	π_2^+
$9a_1$	5.63	9.22	13	0	78	0	3	0	5	1	d_{z^2}
$5b_2$	6.05	9.83	0	0	79	0	0	0	18	5	d_{yz}
$7b_1$	6.50	9.85	0	0	81	0	1	0	13	5	d_{xz}
$8a_1$	6.64	10.30	2	0	83	0	1	0	10	4	$d_{x^2-y^2}$
$6b_1$	7.78	10.46	0	2	4	1	42	0	38	13	π_1^-
$4a_2$	8.00	10.92	0	0	50	0	9	0	36	5	$(d_{xy}-\pi_2^-)^b$
$7a_1$	8.57	11.20	11	0	−1	0	28	0	36	26	π_1^+
$10a_g$	0.41	−0.89	44	0	10	−2	33	−3	12	6	π_3^+
$8b_u$	1.29	−1.20	0	19	0	0	35	1	41	4	π_3^-
$6b_g$[a]	1.62	−1.14	0	0	32	0	0	2	62	4	$(d_{xz}-\pi_2^-)^{ab}$
$5a_u$	5.37	8.03	0	5	0	0	1	2	90	2	π_2^+
$9a_g$	5.55	9.17	12	0	78	0	3	0	6	1	$d_{x^2-y^2}$
$5b_g$	5.86	9.80	0	0	96	0	0	0	1	3	d_{yz}
$8a_g$	6.24	9.98	2	0	90	0	1	0	2	5	$d_{xy}+d_{x^2}$
$7a_g$	6.81	10.40	1	0	80	0	1	0	12	6	$d_{z^2}+d_{xy}$
$7b_u$	7.74	10.43	0	2	0	1	44	0	43	10	π_1^-
$4b_g$	7.98	10.90	0	0	50	0	9	0	36	5	$(d_{xz}-\pi_2^-)^b$
$6a_g$	8.55	11.18	10	0	−1	0	27	0	36	28	π_1^+

[a] Lowest unoccupied MO. [b] b and ab stand for bonding and antibonding, respectively.

***cis*/*trans*-[Ni(η³-$C_3H_5)_2$]**. Data reported in Table 2 confirm that the electronic structures of the isomers are very similar and support the hypothesis that PE[6] and ET[25] spectra could actually be the sum of the spectra of the cis and trans forms, coexisting in the gas phase.

In the energy range 7.5−12 eV the PE spectrum of **A** includes six, quite broad bands (**1**, **2**, **3**, **4**, **5**, and **6** in Figure 4);[26] moreover, evident shoulders are present on the higher IE side of bands **4** and **5**. To our knowledge,

(24) In the free allyl radical the π_1 MO is totally C−C bonding, without nodes along the allyl skeleton, and it is occupied; the π_2 level has a C−C nonbonding nature, it has a single node on the central C2 atom, and it is half-occupied; finally, the π_3 orbital is totally C−C antibonding, it has two nodes along the allyl skeleton, and it is empty.

(25) Guerra, M.; Jones, D.; Distefano, G.; Torroni, S.; Foffani, A.; Modelli, A. *Organometallics* **1993**, *12*, 2203. In this contribution are also reported the results of Xα-SW calculations pertaining to *trans*-[M(η³-$C_3H_5)_2$], M = Ni and Pd, even though no GS MO energy ordering is given.

Table 4. Atomic Character for *cis*-[Pt(η^3-C_3H_5)$_2$] and *trans*-[Pt(η^3-C_3H_5)$_2$][a]

	eigenvalue		population,%								
			Pt			2C2		4C1			
MO	$-\epsilon$/eV	−IE/eV	s	p	d	s	p	s	p	10H	character[b]
$8b_1$	0.23	−2.30	0	0	7	0	41	2	40	10	π_3^-
$5a_2$	0.97	−1.78	0	0	32	0	0	3	62	3	$(d_{xy}-\pi_2^-)^{ab}$
$10a_1$[a]	1.37	−1.19	6	18	9	−1	42	0	19	7	π_3^+
$6b_2$	5.24	8.02	0	5	39	0	1	1	51	4	$(d_{yz}-\pi_2^+)^{ab}$
$9a_1$	5.66	9.31	18	0	77	0	2	0	2	1	d_{z^2}
$5b_2$	6.13	9.52	0	2	56	0	0	1	38	3	$(d_{yz}-\pi_2^+)^b$
$7b_1$	6.65	9.86	0	1	75	0	1	0	16	7	d_{xz}
$8a_1$	6.78	10.22	5	0	76	0	4	0	12	3	$d_{x^2-y^2}$
$6b_1$	7.85	10.53	0	4	4	1	40	0	36	15	π_1^-
$4a_2$	8.26	11.09	0	0	40	0	13	0	40	7	$(d_{xy}-\pi_2^-)^b$
$7a_1$	8.78	11.40	16	0	−2	0	23	0	34	29	π_1^+
$10a_g$	0.32	−1.42	42	0	12	−3	39	−4	7	7	$6s + \pi_3^+$
$6b_g$	0.91	−1.85	0	0	33	0	0	2	61	4	$(d_{xz}-\pi_2^-)^{ab}$
$8b_u$[a]	1.61	−0.93	0	16	0	0	36	2	40	6	π_3^-
$9a_g$	5.50	9.21	16	0	79	0	1	0	3	1	$d_{x^2-y^2}$
$5a_u$	5.58	8.26	0	7	0	0	1	2	88	2	π_2^+
$5b_g$	5.65	9.42	0	0	95	0	0	0	1	4	d_{yz}
$8a_g$	6.16	9.68	4	0	86	0	2	0	2	6	$d_{z^2} + d_{xy}$
$7a_g$	7.00	10.32	3	0	74	0	4	0	14	5	$d_{z^2} + d_{xy}$
$7b_u$	7.84	10.53	0	5	0	1	42	0	41	11	π_1^-
$4b_g$	8.23	11.07	0	0	41	0	12	0	40	7	$(d_{xz} - \pi_2^-)^b$
$6a_g$	8.77	11.39	15	0	−2	0	23	−1	34	31	π_1^+

[a] Lowest unoccupied MO. [b] b and ab stand for bonding and antibonding, respectively.

the origin of these shoulders has never been discussed. The spectrum is best divided in two regions: one extending from 7.5 to 9 eV and including, according to the assignment of Li et al.,[6a] ionizations from Ni-based MOs (the whole band envelope **1**−**3**); the other ranging from 9 to 12 eV and characterized by the presence of bands (**4**−**6**) mainly related to L-based orbitals. Li et al.[6a] also recorded high-resolution He I and He II spectra of the low-IE region evidencing an additional peak, labeled **2A**.

Switching from the He I (21.22 eV) to the He II (40.81 eV) ionizing source, the relative intensity of bands changes as follows: the higher IE side of band **1** (7.64 eV) markedly increases; band **2A** (7.95 eV) does not show significant variations, while the higher IE side of band **2** (8.15 eV) decreases; finally, band **3** (8.52 eV) is scarcely affected. The remaining bands **4**, **5**, and **6** (9.38, 10.36, and 11.48 eV, respectively) decrease in relative intensity, especially bands **5** and **6**.

Within the Gelius model,[27] the cross section of an individual MO is proportional to the sum of the atomic subshell photoionization cross sections of its components weighted by the probability (approximately the orbital composition) of finding in the *j*th MO an electron belonging to the *n*th AO. In this habit, relative intensity variations with the ionizing source energy can be used as an experimental tool to gain information about the MO localization.[28]

Among the MOs included in Table 2, the deepest in energy are the $7a_1-6b_1$ orbitals of *cis*-**A** and the $6a_g-7b_u$ levels of *trans*-**A**. These MOs are almost completely localized on the C $2p_\pi$ AOs; furthermore, their TSIEs are very similar (see Figure 4). According to that and to the He I/He II relative intensity variations of bands **6** and **5**, we confidently assign them to the ionization from the $7a_1/6a_g$ MOs (both related to the π_1^+ $(C_3H_5)_2$ FMO) and the $6b_1/7b_u$ MOs (both related to the π_1^- $(C_3H_5)_2$ FMO), respectively. Incidentally, the assignment of band **5** to two ionization events is consistent with the pronounced shoulder well evident on its higher IE side.

We already remarked that the relative intensity decrease of band **4** with increasing photon energies is less evident than that corresponding to bands **5** and **6**. This evidence implies that ionizing processes hidden under band **4** involve MOs having a sizable participation of Ni 3d AOs. Both in *cis*- and *trans*-**A**, close in energy to the orbitals related to π_1^+ and π_1^- FMOs, there is an orbital ($4a_2$ and $4b_g$ in Table 2) corresponding to the bonding interaction between Ni $3d_\pi$ AOs ($3d_{xy}$ in *cis*-, $3d_{xz}$ in *trans*-**A**) and the $(C_3H_5)_2$ π_2^- combination (see Figure 5). Li et al.[6a] and Guerra et al.[25] evaluated for the corresponding MO of *trans*-**A** a Ni $3d_\pi$ localization ≥ 70%, while, in better agreement with He I/He II relative intensity variations, our calculations estimate a participation of $3d_{xy}$ (in cis) and $3d_{xz}$ (in trans) AOs not exceeding 55%. Analogously to band **5**, the assignment of band **4** to two MOs (the $4a_2$ and $4b_g$ levels) is in tune with the presence of the unresolved band on its higher IE side.

We turn now to examine the IE region including the band envelope **1**−**3**, extending from 7.5 to 9 eV and which has to be associated with the ionization from 10 orbitals (five for each isomer). Among them, eight MOs are mainly localized on the Ni 3d AOs, while the remaining two are reminiscent of the $(C_3H_5)_2$ π_2^+ FMOs. Because electron relaxation phenomena are larger for Ni 3d-based than L-based MOs, the MO energy ordering in GS and TSIE calculations is different (see Table 2), at variance with Xα-SW results of Li et al.[6,25] Furthermore, relaxation effects are larger for the trans isomer, where the atom-like character of Ni 3d-based MOs is stronger. As a final result, the levels with the lowest TSIE in cis and trans arrangements have a different nature: the $6b_2$ MO is almost completely localized on the Ni $3d_{yz}$ AO, and it accounts for a weak antibonding interaction with the π_2^+ level, while the $5a_u$ MO is the orbital reminiscent of the π_2^+ FMO. Moreover, the TSIEs of the $5b_2$ (the MO truly related to the π_2^+ FMO in *cis*-**A**) and $5a_u$ levels (see Table 2 and Figure 4) are very close. On this basis, we propose to assign the lower IE side of band **1** to three ionization processes involving the $6b_2$ and $5b_2$ MOs of *cis*-**A** as well as the $5a_u$ level of *trans*-**A**.

Among the remaining seven MOs, all of them with a strong Ni 3d character, the $7a_g$ and $8a_1$ orbitals, both accounting for a M→L back-bonding interaction (the corresponding COOPs are displayed in Figure 6), have quasi-degenerate TSIEs and are well separated in energy from the others (see Table 2 and Figure 4). On this basis, we assign them to band **3**. We do not attempt any detailed assignment of the remaining MOs ($9a_1$ and

(26) Throughout the paper we followed the labeling scheme adopted by Li et al.[6a] Moreover, it deserves to be mentioned that the lack of any sharp feature in the PE spectrum of **A** was ascribed by Batich[6g] to the lack of rigidity of the molecule and to the probable presence of different isomers in the gas phase.

(27) Gelius, U. *Electron Spectroscopy*; Shirley, D. A., Ed.; North-Holland: Amsterdam, 1972; p 311.

(28) The C and H valence atomic subshell photoionization cross sections significantly decrease on passing from the He I to the He II ionizing source ($\sigma_{C_{2s}}$(He I), $\sigma_{C_{2s}}$(He II), $\sigma_{C_{2p}}$(He I), $\sigma_{C_{2p}}$(He II), σ_H(He I), σ_H(He II) are 1.230, 1.170, 5.128, 1.875, 1.888, 0.2892 Mb).[29] At variance with that the Ni, Pd and Pt *n*d AOs show an opposite behavior ($\sigma_{Ni_{3d}}$(He I), $\sigma_{Ni_{3d}}$(He II), $\sigma_{Pd_{4d}}$(He I), $\sigma_{Pd_{4d}}$(He II), $\sigma_{Pt_{5d}}$(He I), $\sigma_{Pt_{5d}}$(He II) are 3.984, 8.367, 26.05, 32.52, 29.46, 31.33 Mb).[29]

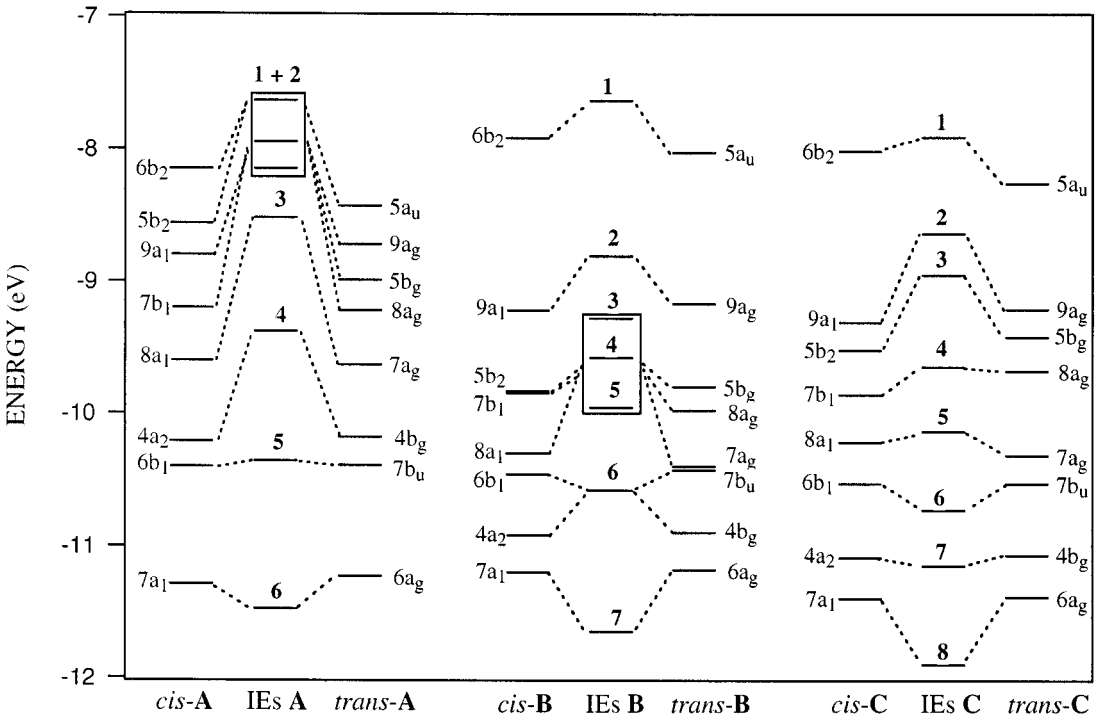

Figure 4. Comparison between TSIEs for *cis*- and *trans*-[M(η^3-C_3H_5)$_2$] (M = Ni (**A**), Pd (**B**), Pt (**C**)) and corresponding experimental IEs. Bands for which a detailed assignment has not been attempted (see text) are enclosed in a box.

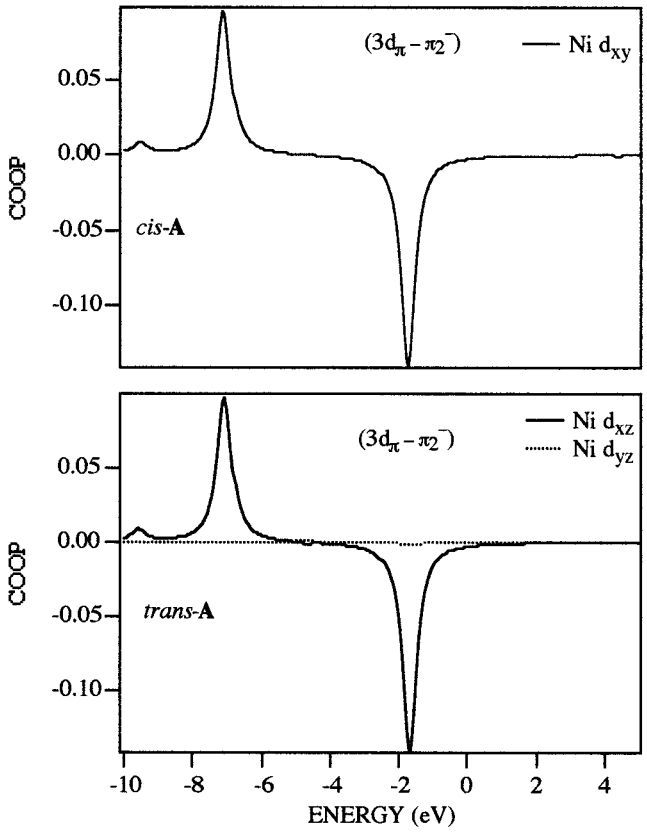

Figure 5. COOP between the (C_3H_5)$_2$ π_2^- FMO and Ni 3d$_\pi$ AOs for the (a) cis and (b) trans isomer. Bonding (antibonding) states are represented by positive (negative) peaks.

7b$_1$ in *cis*-**A**, 9a$_g$, 5b$_g$, and 8a$_g$ in *trans*-**A**) which are hidden under band **2** and the higher IE side of band **1**.

The relief of symmetry constraints on passing from the C_{2h} to the C_{2v} structure does not limit its influence on the occupied MOs, but it affects the MO ordering of virtual levels too. In particular, the MOs reminiscent of π_3^+ and π_3^- FMOs have, in the cis complex, the same order of the optimized *cis*-(C_3H_5)$_2$ fragment, while the opposite is true for the trans isomer (see Figure 3 and Table 2). A closer look at Table 2 provides an explanation of this finding. The π_3^- FMO of *trans*-(C_3H_5)$_2$ is stabilized by the mixing with empty, ungerade Ni 4p AOs, while the corresponding level in *cis*-(C_3H_5)$_2$ is only destabilized by a weak interaction with the occupied Ni 3d$_{xz}$ AO. As far as the π_3^+ FMO is concerned, the stabilizing admixture with empty 4p Ni AOs is symmetry allowed only in *cis*-**A**.

The ET spectrum of **A** consists of three resonances (0.49, 1.17, and 2.04 eV) ascribed by Guerra et al.[25] to electron capture processes involving MOs related to π_2^-, π_3^+, and π_3^- FMOs. This is in tune with the presence, both in *cis*-**A** and *trans*-**A**, of three low lying empty orbitals (see Table 2), mainly localized on the (C_3H_5)$_2$ fragment and related to π_2^-, π_3^+, and π_3^- FMOs. TSAE values are found in the correct energy range;[30] nevertheless, differential relaxation phenomena give rise to a TSAE spectrum that does not allow any confident assignment of ET resonances.[32] This seems to indicate

(29) Yeh, J. J.; Lindau, I. Atomic Subshell Photoionization Cross Section and Asymmetry Parameters: $1 \le Z \le 103$. *At. Data Nucl. Data Tables* **1985**, *32*, 1.

(30) Venuti and Modelli[31] recently performed a series of Hartree−Fock calculations by using the exponent stabilization method to distinguish the virtual orbitals associated with temporary anion states. For the cases they considered, the agreement between orbital energies and observed resonances was not completely satisfactory.

(31) Venuti, M.; Modelli, A. *J. Chem. Phys.* **2000**, *113*, 2159.

(32) The theoretical evaluation of AEs seems to require highly flexible basis sets.[33] As a test, we have run a further series of calculations on *cis*-and *trans*-**A** by using a triple-ζ STO basis for all the atoms. The cis isomer is found to be less stable than the trans one by 0.13 kcal/mol, and geometries agree with previous ones within 0.005 Å (for BL) and 0.1° (for BA). TSAEs of the 5a$_2$ and 6b$_g$ MOs are 1.18 and 1.27 eV, respectively.

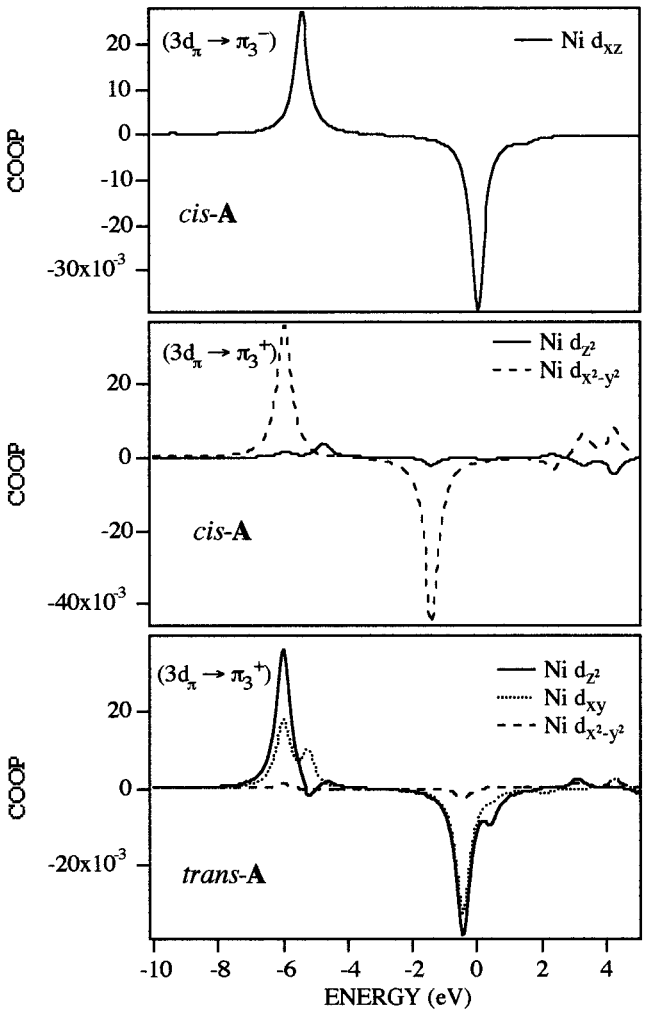

Figure 6. COOP between the $(C_3H_5)_2$ π_3^+/π_3^- FMOs and Ni $3d_\pi$ AOs for the (a) cis and (b) trans isomer.

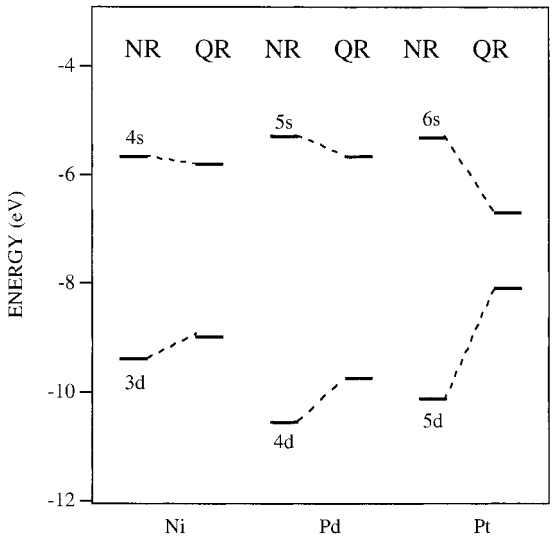

Figure 7. *n*s and (*n*−1)d atomic energy levels of the Ni triad evaluated at the nonrelativistic (NR) and quasirelativistic (QR) level. The $(n-1)d^8ns^2$ configuration was used in all the calculations.

that the adopted procedure is able to provide only a semiquantitative estimate of experimental AEs.

***cis/trans*-[Pd(η^3-C_3H_5)$_2$]**. The PE spectrum of **B** includes seven bands (**1**−**7** in Figure 4) in the 7.5−12 eV energy range.[6] As done for **A**, we divide it in three regions: the first extending from 7.5 to 9 eV and including only two well-resolved and asymmetric peaks (ΔIE_{2-1} = 1.17 eV; ΔIE_{3-2} = 0.47 eV); the second covering the IE region from 9 to 10 eV and characterized by the presence of bands **3**, **4**, and **5**; the third comprising the rest of the spectrum, i.e., bands **6** and **7**. An evident shoulder, never discussed before, is present on the higher IE side of band **7**. Also in this case, Li et al.[6a] recorded a high-resolution He I spectrum of the first IE region. The authors claimed that the fitting of the two peaks therein present with two components was inadequate as a consequence of the peak asymmetry. Concomitantly, they pointed out that the best fit with the least number of components was that expected for a vibrational progression with frequencies varying from 1150 to 1300 cm^{-1}.

Moving from the He I to higher energy sources (32, 50, 72, and 90 eV), the relative intensity of bands **1**−**7** has the following behavior: band **1** (7.64 eV) dramatically decreases, bands **2**−**5** (8.81, 9.28, 9.58, 9.96 eV, respectively) increase, while bands **6** and **7** (10.58 and 11.65 eV, respectively) decrease, the latter much more than the former.

Our theoretical outcomes (see Table 3) confirm once again the close similarity of the electronic structure of cis and trans isomers, while the comparison of data reported in Tables 2 and 3 stresses significant differences between **A** and **B**: (i) the different character of the GS HOMO in *trans*-**A** and *trans*-**B**; (ii) the presence, in **B**, of two high lying levels well distinct in energy from the remaining ones; (iii) the energy position of the MO accounting for the $d_\pi-\pi_2^-$ bonding interaction.

In both *cis*-**B** and *trans*-**B** the GS HOMO ($6b_2$ and $5a_u$ levels, respectively) is localized on the (η^3-C_3H_5)$_2$ fragment and is reminiscent of the π_2^+ FMO. This is the result of several, concurring factors: (i) the lower energy of the Pd 4d AOs with respect to the Ni 3d ones (see Figure 7); (ii) the destabilizing participation of occupied Pd 4d AOs to the $6b_2$ MO is larger than that of the Ni 3d AOs to the $5b_2$ MO; (iii) the stabilizing participation of unoccupied Pd 5p AOs to the $6b_2$ and $5a_u$ MOs is smaller than that of the Ni 4p AOs to the $5b_2$ and $5a_u$ orbitals. The marked decrease of band **1** with the photon energy increase allows us to confidently assign it to the ionization from the ligand-based GS HOMO of *cis*- and *trans*-**B**.

We already mentioned that Li et al.[6a] ascribed the asymmetry of band **1** to a vibrational progression with frequencies in the range 1150−1300 cm^{-1}, quite close to the C−C−C symmetric stretch frequencies (ν^s_{C-C-C}, 1009−1010 cm^{-1}) of solid *trans*-**B**.[34,35] To verify this interpretation, we carried out a further series of numerical experiments to evaluate vibrational frequencies of *trans*- and *cis*-**B** (VIB(GS)) as well as of the ^2A_u and $^2B_2$ electronic states at the corresponding optimized geometries (VIB(^2A_u) and VIB($^2B_2$)).[36] The obtained results (see Table 5) indicate that the blue-shift under-

(33) Ziegler, T. *Can. J. Chem.* **1995**, *73*, 743.
(34) Andrews, D. C.; Davidson, G. J. *J. Organomet. Chem.* **1973**, *55*, 383.
(35) When considering [M(η^3-C_3H_5)$_2$], the C_3H_5 V^s_{C-C-C} gives rise to in-phase (a_1/a_g) and out-of-phase (b_1/b_u) linear combinations.

Table 5. Vibrational Frequencies (cm⁻¹) Corresponding to In-Phase (+) and Out-of-Phase (−) Combinations of V^{s}_{C-C-C} for *cis*- and *trans*-Pd(η³-C₃H₅)₂

	VIB(GS)			
	cis	trans	VIB($^2B_2$)	VIB(^2A_u)
+	1007	1009	1013	1014
−	1006	1005	1004	1008

gone by ν^{s}_{C-C-C} upon ionization of the $5a_u$ and $5b_2$ MOs in *trans*- and *cis*-**B**, respectively, is negligible. This means that vibrational progressions might be present, but the evaluation of their frequencies should be based on the assumption that band **1** is due to two ionization events.

Among PE bands associated with the ionizations from Pd-based MOs, band **2** is well distinct in energy from bands **3**, **4**, and **5** (see Figure 4). Moreover, its intensity decreases relative to that of bands **3**, **4**, and **5** with increasing photon energies.[6a] Accordingly, Li et al.[6a] associated band **2** with the ionization from the Pd-based MO having the lowest Pd 4d contribution, i.e., in our calculations, the $9a_g$ and $9a_1$ MOs. This is confirmed by comparing experimental (ΔIE_{2-1} and ΔIE_{3-2} are 1.17 and 0.47 eV, respectively) and theoretical ($\Delta TSIE_{9ag-5au}/\Delta TSIE_{9a1-6b2}$ and $\Delta TSIE_{5bg-9ag}/\Delta TSIE_{5b2-9a1}$ are 1.14/1.30 and 0.63/0.61 eV, respectively) data. Analogously to the **A** case, we do not attempt any detailed assignment of bands **3**−**5**, which, as a whole, are associated with the ionizations from the $5b_g$, $8a_g$, and $7a_g$ MOs of *trans*-**B** as well as from the $5b_2$, $7b_1$, and $8a_1$ orbitals of *cis*-**B** (see Figure 4).

Moving to bands **6** and **7**, they both decrease in relative intensity with increasing photon energies, but such a behavior is much more marked for band **7**. The inspection of Table 3 provides a rationale of it. Band **6** is actually due to the ionization from MOs having some parentage with the π_2^- (the $4b_g$ and $4a_2$ levels) and π_1^- (the $7b_u$ and $6b_1$ orbitals) FMOs, and the former pair has a sizable participation of Pd $4d_\pi$ AOs (they account for the main source of bonding between the Pd atom and the $(\eta^3\text{-}C_3H_5)_2$ moiety). At variance with that, band **7** includes only ionization processes involving L-based MOs (the $6a_g$ and $7a_1$ levels, both related to the π_1^+ FMO) having a strong C $2p_\pi$ character.

In agreement with experiment, the TSIEs of π_1^- and π_1^+ (see Tables 2 and 3) are only slightly modified on passing from **A** to **B**, while the opposite is true when dealing with π_2^-, which is, both in *cis*-**B** and in *trans*-**B**, more stable than π_1^-. This is quite unexpected if we consider that (i) π_2^- is empty in the free $(C_3H_5)_2$ fragment and (ii) the Pd 4d AOs are lower in energy than the Ni 3d ones (see Figure 7). On the other hand, the IEs of the $4b_g/4a_2$ MOs seem to indicate that the overlap between the diffuse Pd $4d_\pi$ AOs and the π_2^- FMO plays a more important role than the frontier orbital energy matching. According to that, the Hirshfeld[37] atomic charge of Ni in *cis*/*trans*-**A** (0.30/0.29) is significantly smaller than that of Pd in *cis*/*trans*-**B** (0.43/0.42).

Finally, as already remarked when assigning bands **4** and **5** in **A**, the association of band **7** in **B** to two ionization events is consistent with the presence of an evident shoulder on its IE side.[6]

The ET spectrum of **B** is very similar to that of **A**. Actually, the energy range extending from 0 to 3 eV includes three resonances (0.46, 1.12, and 2.17 eV), which Guerra et al.[25] assigned to MOs related to π_2^-, π_3^+, and π_3^- FMOs. According to that, we find (see Table 3) that the three lowermost unoccupied MOs of *cis*-**B** and *trans*-**B** are reminiscent of π_2^-, π_3^+, and π_3^- FMOs. Analogously to **A**, TSAEs lie in the correct energy range, but, as a consequence of extended differential relaxation effects, ET resonances cannot be safely assigned to specific MOs. In this regard, it has to be emphasized that the energy relaxation computed for the $10a_g$ MO of *trans*-**B**, possessing a high Pd 5s character, is about half that of the other empty levels included in the table.

***cis/trans*-[Pt(η³-C₃H₅)₂]**. The 7.5−12 eV IE region of the PE spectrum of **C** consists of eight bands (**1**−**8** in Figure 4),[6a] i.e., a band for each of the occupied MOs expected in the molecular valence manifold. We divide this energy region in the same three zones we have chosen in the case of **B**. The first extends from 7.5 to 9 eV, and it now includes three well-resolved peaks, the first and the third being clearly asymmetric; the second covers the 9−10 eV energy range, and it consists of two bands, while the third includes the rest of the spectrum.

Switching from the He I to higher energy sources (40, 50, 60, and 70 eV), the relative intensity of bands **1**−**8** has the following behavior: band **1** (7.91 eV) dramatically decreases; bands **2**−**5** (8.64, 8.95, 9.65, 10.14 eV, respectively) increase, even if band **3** less than the others; bands **6**, **7**, and **8** (10.73, 11.15, and 11.90 eV, respectively) decrease. In this regard, we point out that in the PE spectra recorded at 40, 50, 60, and 70 eV (see Figure 6 of ref 6a) band **7** undoubtedly decreases much less than bands **6** and **8**.

Moving to our calculations, we first want to stress that, as in the previous cases, the TSIEs pertaining to occupied MOs are very similar in cis and trans isomers. Furthermore, the presence of a band (the first) assigned in both **B** and **C**[6a] to a L-based MO (see above its relative intensity behavior with photon energies) followed by two peaks whose ΔIE decreases on passing from **B** to **C** (see Table 4 and Figure 4) is well reproduced.[38] The MOs with the lowest TSIEs correspond in both *trans*-**C** and *cis*-**C** to the ligand-based π_2^+ FMO (the $5a_u$ and $6b_2$ orbitals, respectively), and they should be attributed to band **1**. In this regard, it should be noted that the energy position of the $6b_2$ MO is slightly higher than that of the $5a_u$ one because the destabilizing interaction with occupied Pt 5d AOs is prevented by symmetry in the trans form. This could explain the asymmetry of the peak.

In both isomers the orbital with the second lowest TSIE ($9a_1$ and $9a_g$) is almost completely localized on the

(36) The geometries relative to the ^2A_u and $^2B_2$ electronic states as well as the corresponding vibrational parameters have been computed by running spin-polarized calculations. Results indicate that Pd−C BLs are significantly longer in the ionic state (BL_{Pd-C1}/BL_{Pd-C2} computed for the ^2A_u and $^2B_2$ electronic states are 2.262/2.170 and 2.247/2.147 Å, respectively) than in the GS (see Table 1). In contrast to that, the BL_{C1-C2} (1.410 and 1.413 Å in ^2A_u and $^2B_2$, respectively) is scarcely affected by the removal of an electron from the $6b_2$ and $5a_u$ MOs, both C1−C2 nonbonding in character.

(37) (a) Hirshfeld, F. L. *Theor. Chim. Acta* **1977**, *44*, 129. (b) Wiberg, K. B.; Rablen, P. R. *J. Comput. Chem.* **1993**, *14*, 1504.

(38) The experimental decrease of ΔIE_{2-1} on passing from **B** to **C** is theoretically reproduced only for *trans*-**C**: $\Delta IE_{2-1} = 0.73$ eV, $\Delta TSIE_{2-1} = 0.95/1.29$ eV in *trans*/*cis*-**C**; $\Delta IE_{3-2} = 0.31$ eV, $\Delta TSIE_{3-2} = 0.21$ eV in both *trans*- and *cis*-**C**.

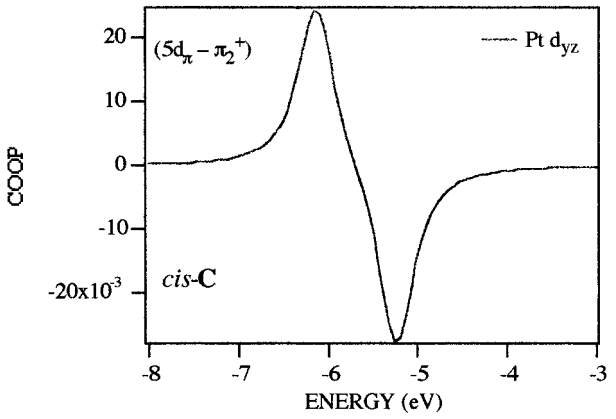

Figure 8. COOP between the $(C_3H_5)_2$ π_2^+ fragment MO and Pt $5d_{yz}$ AOs for *cis*-**C**.

Pt atom (95% in both cases, see Table 4). Consistently, the relative intensity of band **2** dramatically increases with the photon energy.

Two ionizing processes are hidden under band **3**, one of them involving a MO of *cis*-**C** (the $5b_2$ level) with a significant (42%) localization on the $(\eta^3\text{-}C_3H_5)_2$ fragment and accounting for a weak π-bonding interaction between the Pt $5d_{yz}$ and the π_2^+ FMO (see the corresponding COOP in Figure 8). This explains why band **3** increases in relative intensity much less than bands **2**, **4**, and **5** when the photon energy is increased.

Moving to the assignment of bands **4** and **5**, it has to be remarked that the $7b_1$ and $8a_1$ MOs of *cis*-**C** have a comparable Pt 5d character. In contrast to that, the localization of the $8a_g$ orbital on Pt AOs (90%) is definitely higher than that of the $7a_g$ one (77%). This is consistent with the assignment of band **4** to the ionization from $7b_1$ and $8a_g$ MOs, while ionizing processes involving the $7a_g$ and $8a_1$ levels are hidden under band **5**, whose intensity decreases with respect to band **4**. Relative intensity variations of bands **3** and **5** coupled to the observation of the evident asymmetry of the former represent, in our opinion, a clear proof of the coexistence of cis and trans complexes in the gas phase.

The third region of the PE spectrum of **C** includes three bands that, with the same arguments invoked for **A** and **B**, can be confidently assigned to the ionization from $(\eta^3\text{-}C_3H_5)_2$ π_1^+, π_1^-, and π_2^- FMOs. We already stressed that band **7** decreases in relative intensity less than bands **6** and **8** when the energy of the ionizing source increases. This is an experimental evidence that under this band are hidden ionizing processes involving MOs with a sizable Pt 5d character, i.e., the $4a_2$ and $4b_g$ MOs, which account for the main source of $M-(\eta^3\text{-}C_3H_5)_2$ bonding. In close agreement with experiment, the quasi-degenerate $4a_2$ and $4b_g$ orbitals of *cis*-**C** and *trans*-**C** lie at lower energy than corresponding MOs in *cis*-**B** and *trans*-**B** as a consequence of the better energy matching (see Figure 7) between Pt 5d AOs and the empty π_2^- FMO. The assignment of bands **6** and **8** to the ionization from orbitals reminiscent of the π_1^- ($6b_1$/$7b_u$ MOs) and π_1^+ ($7a_1$/$6a_g$ MOs) FMOs, respectively, is straightforward.

Although the interaction between d_π M AOs and π_2^- FMO is stronger in Pt than in Pd, the Hirshfeld[37] atomic charge of Pt in *cis*/*trans*-**C** (0.28/0.25) is significantly smaller than that of Pd. This is easily explained by referring to the composition of the $6a_g$ and $7a_1$ MOs, which are characterized by a significant participation of the Pt 6s AO, lowered in energy by relativistic effects (see Figure 7).

The ET spectrum of **C** in the 0−3 eV energy region is very similar to those of **A** and **B**, and it includes three resonances at 0.65, 1.41, and 2.30 eV.[25] Also in this case, the three lowermost unoccupied MOs of **C** have a significant participation of the C $2p_\pi$ AOs (see Table 4) and are related to the π_2^-, π_3^+, and π_3^- FMOs. Nevertheless, as a consequence of relativistic effects, their energy ordering is different from that of **A** and **B**. In this regard, we should consider that (i) even in GS calculations, the $6b_g$/$5a_2$ MOs, both $d_\pi-\pi_2^-$ antibonding in character, are not the LUMOs any more; (ii) analogously to *trans*-**B**, the $10a_g$ MO has a high localization on the M *n*s AO, and its GS energy (−0.32 eV) is higher than that of the corresponding level in **A** and **B** (−0.44 and −0.41 eV, respectively); (iii) relaxation phenomena undergone by the $10a_g$ MO upon electron capture are smaller than in **A** but larger than in **B**.

The numerical agreement between TSAEs and experimental AEs is probably better in **C** than in **A** and **B**; nevertheless, to attribute specific MOs to the three experimental resonances of the ET spectrum of **C** would be a matter of taste, and on this basis, we do not attempt any detailed assignment of ETS data pertaining to **C**.

Conclusions

In this contribution we have presented a theoretical investigation of the electronic and molecular structure of the cis and trans isomers of $[M(\eta^3\text{-}C_3H_5)_2]$ (M = Ni, Pd, Pt) complexes. For all molecules, binding energy differences between cis and trans forms are very small (<0.2 kcal/mol). On this basis, discrepancies between theoretical MO ordering of occupied orbitals and gas-phase variable energy PE spectra can be worked out by admitting that cis and trans isomers are present in the gas phase in a comparable amount.

Although the first IE is always related to orbitals of the same symmetry in all the compounds (b_2 for the cis isomer and a_u for the trans one, respectively), the corresponding MO differs in character both when comparing two isomers and when moving along the series. It is a $(\eta^3\text{-}C_3H_5)_2$-based MO in all the trans complexes as well as in *cis*-$[Pd(\eta^3\text{-}C_3H_5)_2]$ and *cis*-$[Pt(\eta^3\text{-}C_3H_5)_2]$. In contrast to that, it is a Ni 3d-based MO in *cis*-$[Ni(\eta^3\text{-}C_3H_5)_2]$. These differences have to be traced back to the different energy and spatial properties of *n*d AOs along the Ni triad. The application of the Slater transition state procedure to the evaluation of AEs provides theoretical values in the correct energy range, though a confident assignment of the ET spectra is not obtained.

Acknowledgment. It is a pleasure to thank Professor Alberto Modelli and Dr. Marco Venuti of the University of Bologna (Italy), Professor Eugenio Tondello of the University of Padova (Italy), and Professor Tom Ziegler of the University of Calgary (Canada) for the insightful discussions.

OM0008427